E3S Web of Conferences **415**, 01004 (2023) https://doi.org/10.1051/e3sconf/202341501004
DFHM8

Factors controlling bed and bank erosion in the Illgraben (CH)

Tjalling de Haas[1*], *Brian* McArdell[2], *Wiebe* Nijland[1], *Amanda* Åberg[1,2], *Jacob* Hirschberg[2], *Steven* de Jong[1], and *Pierre* Huguenin[3]

[1]Department of Physical Geography, Utrecht University, Utrecht, The Netherlands.
[2]Swiss Federal Institute for Forest, Snow and Landscape Research WSL, Birmensdorf, Switzerland.
[3]Swiss Federal Institute for Forest, Snow and Landscape Research WSL, Sion, Switzerland.

Abstract. Debris flows can grow greatly in size and hazardous potential by eroding bed and bank materials. However, erosion mechanisms are poorly understood because debris flows are complex hybrids between a fluid flow and a moving mass of colliding particles, bed erodibility varies between events, and field measurements are hard to obtain. Here, we (i) quantify the spatio-temporal patterns of erosion and deposition and (ii) identify the key controls on debris-flow erosion in the Illgraben (CH). We use a dataset that combines information on flow properties, antecedent rainfall, and bed and bank erosion for 13 debris flows that occurred between 2019 and 2021. We show that spatio-temporal patterns of erosion and deposition in natural debris-flow torrents can be highly variable and dynamic, and we identify a memory effect where erosion is strong at locations of strong deposition during previous flows and vice versa. We find that flow conditions and antecedent rainfall (affecting bed wetness) jointly control debris-flow erosion. We find statistically significant correlations between channel erosion/deposition and a wide range of flow conditions, including frontal flow depth, velocity, and discharge, and flow volume, cumulative shear stress and seismic energy, as well as antecedent rainfall. Overall, flow conditions describing the cumulative forces exerted at the bed during an event, such as cumulative shear stress and flow volume, best explain erosion. A shear-stress approach accounting for bed erodibility may therefore be applicable for modelling and predicting debris-flow erosion. This work can provide input for model development by identifying correlations of flow and bed conditions with erosion that models should oblige.

1 Introduction

The magnitude of a debris flow can increase substantially by basal and bank erosion while it traverses from initiation zone to valley floor resulting in an increase in hazardous potential. In addition, debris flows are increasingly recognised as one of the fundamental physical processes that transport sediment and erode bedrock in mountainous topography. However, limited understanding of the processes that control debris-flow erosion currently limits (i) accurate estimation of debris-flow magnitude and effective hazard mitigation and (ii) understanding and modelling of landscape evolution.

Field data on debris-flow erosion are scarce and its analysis is typically hampered by unknown or irreproducible boundary conditions. There has been a recent increase in the number of numerical models incorporating erosion [1-3], but the inconsistency in erosion rate equations as a result of a lack of a unified theory still results in a disparity of model outcomes. At the same time, erosion is still neglected in many other models actively used for hazard assessment, which leads to systematic underestimation of debris-flow propagation, runout, and impact [4].

In this study we present detailed in-situ measurements of debris-flow conditions, antecedent rainfall, and high-resolution measurements of topographic channel change for 13 debris flows in the Illgraben torrent in the southwestern Swiss Alps. With this data we (i) quantify the spatio-temporal patterns of debris-flow erosion and deposition and (ii) identify the key processes that govern debris-flow erosion and deposition. This abstract combines work by De Haas et al. [5], De Haas et al. [6], and new data.

2 Illgraben catchment and torrent

The Illgraben torrent experiences multiple debris flows each year. These flows are generally triggered by summer storms between May and October. The Illgraben system extends from 610 to 2716 m a.s.l., and consists of dolomites, quartzite, conglomerates, and calcareous sedimentary rocks.

The channel stretching from the Illhorn mountain down to the Rhone River has a length of ~6.5 km, of which the distal 4.8 km hosts 28 check dams which cause vertical drops of several meters along the channel bed (Fig. 1). The reach with check dams has an unconsolidated bed. For the most downstream 2 km the channel traverses a large alluvial fan.

---

* Corresponding author: t.dehaas@uu.nl

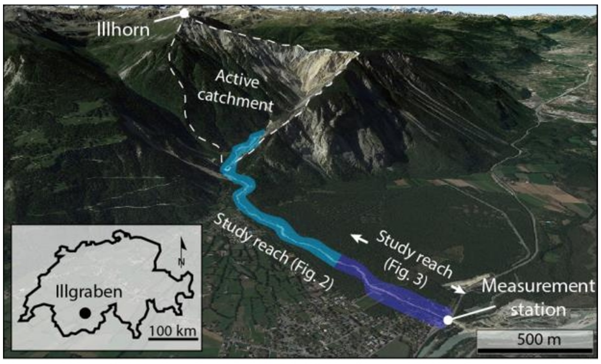

Fig. 1. Overview of the Illgraben catchment, fan, channel, and location of the study reach and measurement station.

3 Methods

3.1 Topographic measurements

We have measured before and after channel topography of the downstream 3.3 km of the channel through drone-based photogrammetry (Fig. 1). Digital elevation models (DEMs) of the study reach were made through structure-from-motion with Agisoft Metashape Pro. The 2019 imagery was captured with a DJI Mavic 2 Pro. These surveys were co-aligned and include 29 ground control points (GCPs) to optimize absolute and relative accuracies [7]. For the 2020 and 2021 surveys a DJI Phantom 4 RTK was used. The real-time kinematic (RTK) technology in this drone ensured higher accuracies [8]. These surveys were processed individually including ~10 GCPs. The absolute and relative accuracies of the DEMs are < 10 cm in xy and z directions, and in the order of 5 cm for most surveys.

3.2 Debris-flow characteristics

Debris-flow characteristics are measured by the Swiss Institute for Forest, Snow and Landscape Research (WSL) at a station at check dam 29 in the Illgraben channel, located near the downstream end of the Illgraben channel approximately 120 m upstream of the confluence with the Rhône River (Fig. 1). The station records flow depth, frontal flow velocity, frontal discharge, flow density, flow volume, normal and shear forces, and seismic ground vibrations [9].

3.3 Antecedent rainfall

Antecedent rainfall was measured at the Swiss Federal Office of Meteorology and Climatology (MeteoSwiss) station located near Crans-Montana at an elevation of 1423 meters above sea level, approximately 11 kilometres from the Illgraben torrent (lat/lon 46.298806°/7.460814°). The antecedent rainfall is defined as the cumulative amount of rainfall in a given period preceding arrival of the debris flow at the measurement station.

4 Results

The 13 studied debris ranged in size from 600 to 87,000 m^3, had frontal flow velocities between 0.5 and 9 $m\ s^{-1}$, frontal flow depths ranging from 0.25 to 3 m, and mean bulk densities between 1600 and 2300 $kg\ m^{-3}$. There is a wide variety in the hydrographs and flow regimes, ranging from (i) single-surge flows with a steep front followed by a tapering tail to (ii) flows with indistinct fronts and (iii) to multi-surge events. Flows range from having well-developed to poorly-developed coarse-grained fronts, and can have hyperconcentrated or muddy-viscous bodies and tails.

4.1 Spatio-temporal patterns of erosion and deposition

The topographic changes within the lowest 3.3 km of the Illgraben channel reveal a strong spatio-temporal heterogeneity in erosion and deposition patterns [5] (Fig. 2). The check dams cause a strong saw-tooth pattern of erosion and deposition, with most deposition or erosion just downstream of the check dams followed by downstream decreases towards near-zero channel elevation change at the crest of the next check dam. The check dams effectively set a local base level at the crest of each dam and generally prevent the channel from laterally migrating. Bed erosion dominates channel erosion, although bank erosion and collapses are commonly observed.

Memory effects affect the spatio-temporal patterns of erosion and deposition. Erosion and deposition in a debris flow often depend on the erosion and deposition by previous debris flows. Localities where substantial deposition occurred have a high probability of substantial erosion during subsequent flow(s) and vice versa (Fig. 2). This might in part be the result of the channel-bed deviating around an equilibrium profile, set by the check dams in the studied reach.

Relatively large flows that exceed the channel capacity form levee and overbank deposits. This can lead to net deposition, despite substantial thalweg erosion, thereby limiting or even counterbalancing further flow bulking as the debris flow traverses further downstream.

4.2 Factors controlling erosion and deposition

Multiple flow properties have statistically significant correlations with channel-bed elevation change in the lowest 800 m of the channel [6], when ignoring one or two common outliers (Fig. 3). These outliers, events 8 and 11, are the result of a very long flow duration or limited antecedent rainfall, respectively.

The strongest correlations in our dataset (excluding event 11) are those between channel-bed elevation change and flow properties that consider debris-flow activity over time, such as flow volume (R^2 = 0.58), cumulative shear stress (R^2 = 0.55), and seismic energy (squared integrated ground velocity amplitude) (R^2 = 0.41).

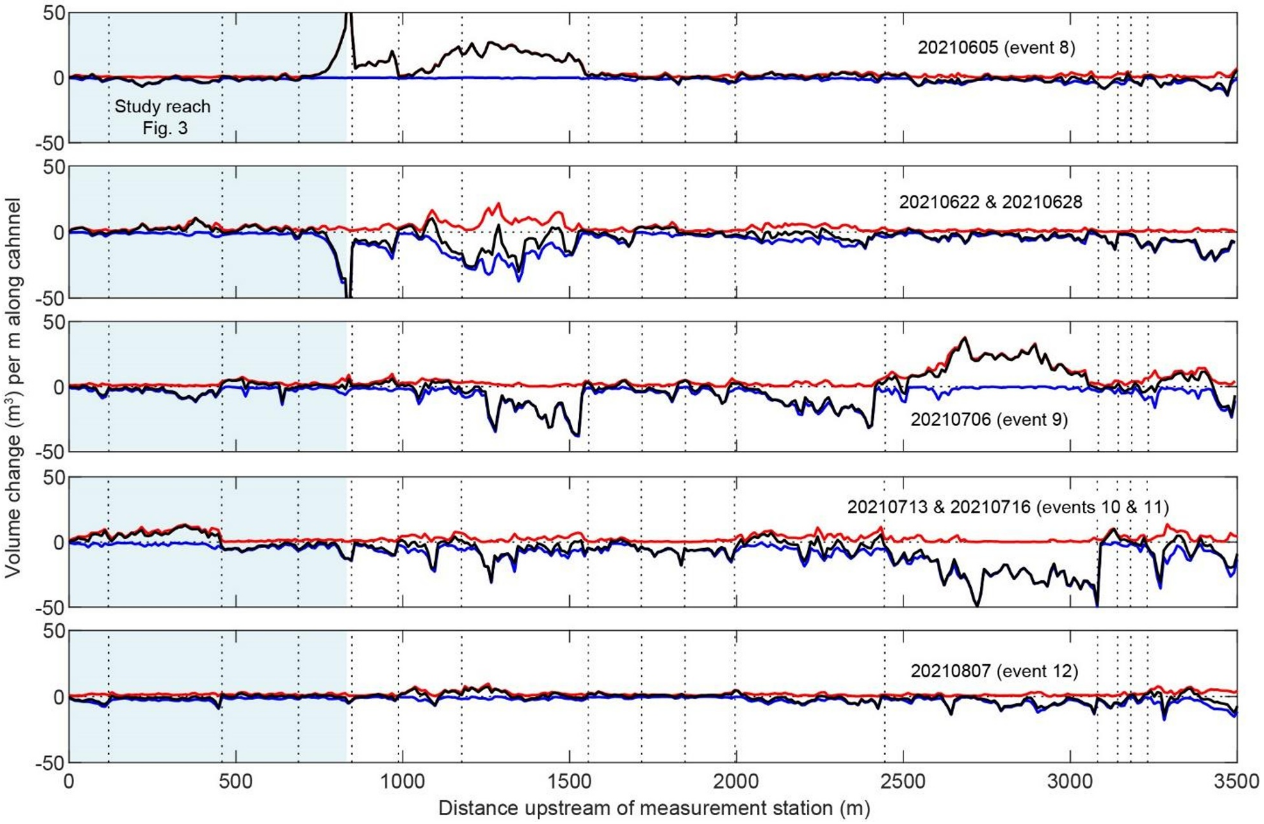

Fig. 2. Examples of spatio-temporal patterns of erosion and deposition. The red, blue, and black lines indicate the volumes of deposition, erosion, and the net volume change per meter along channel, respectively. The dashed lines indicate the locations of the check dams that affect the channel. The blue fill indicates the study reach for the data shown in Fig. 3. Note the pronounced memory effects around distances of 1200 and 2500 m upstream of the measurement station.

Statistically significant relations are also found for frontal flow properties when we exclude events 8 and 11: frontal flow depth ($R^2 = 0.39$), frontal flow velocity ($R^2 = 0.46$), and frontal discharge ($R^2 = 0.42$). We find no significant trend between mean bulk density and channel-bed elevation change (Fig. 3e), although some high-density flows seem to have a higher tendency towards deposition.

We further find statistically significant positive correlations between antecedent rainfall over a period of 2-3 hours, when excluding event 8 ($R^2 \approx 0.47$; $p \approx 0.01$) (Fig. 3i). For a period of 4-12 hours, the correlation decreases in strength and becomes marginally significant, while beyond a period of 12 hours there is no significant trend. Similarly, we find no significant trend for 1-hour antecedent rainfall. We attribute the strong correlation between short-term antecedent rainfall and channel-bed elevation change to an increase in bed moisture, and thus erodibility, with increasing antecedent moisture [10].

5 Discussion

Our observations highlight the complexity of debris-flow erosion and deposition. We show that the spatio-temporal patterns of erosion and deposition can be heterogeneous, partly induced by memory effects. We further show that both flow and bed conditions significantly affect erosion and thereby flow-volume growth, but that none of the variables has a very high predictive capacity on its own. Both flow and bed conditions should therefore be considered in prediction and modelling of debris-flow erosion, in contrast to previous work which predominantly attributes erosion to either flow properties [11] or bed wetness [12]. The material eroded by a debris flow depends most strongly on the cumulative forces exerted on the bed during the entire event in our dataset. Predictions should therefore account for the forces exerted on the channel bed during the entire event. Our data further shows that shear forces and particle-impact forces are strongly correlated and jointly erode the bed, i.e., flows with higher shear forces also have higher impact forces. This suggest that a shear stress approach accounting for bed erodibility may suffice to model debris-flow. This work provides guidelines and data against which to validate and calibrate debris-flow erosion models.

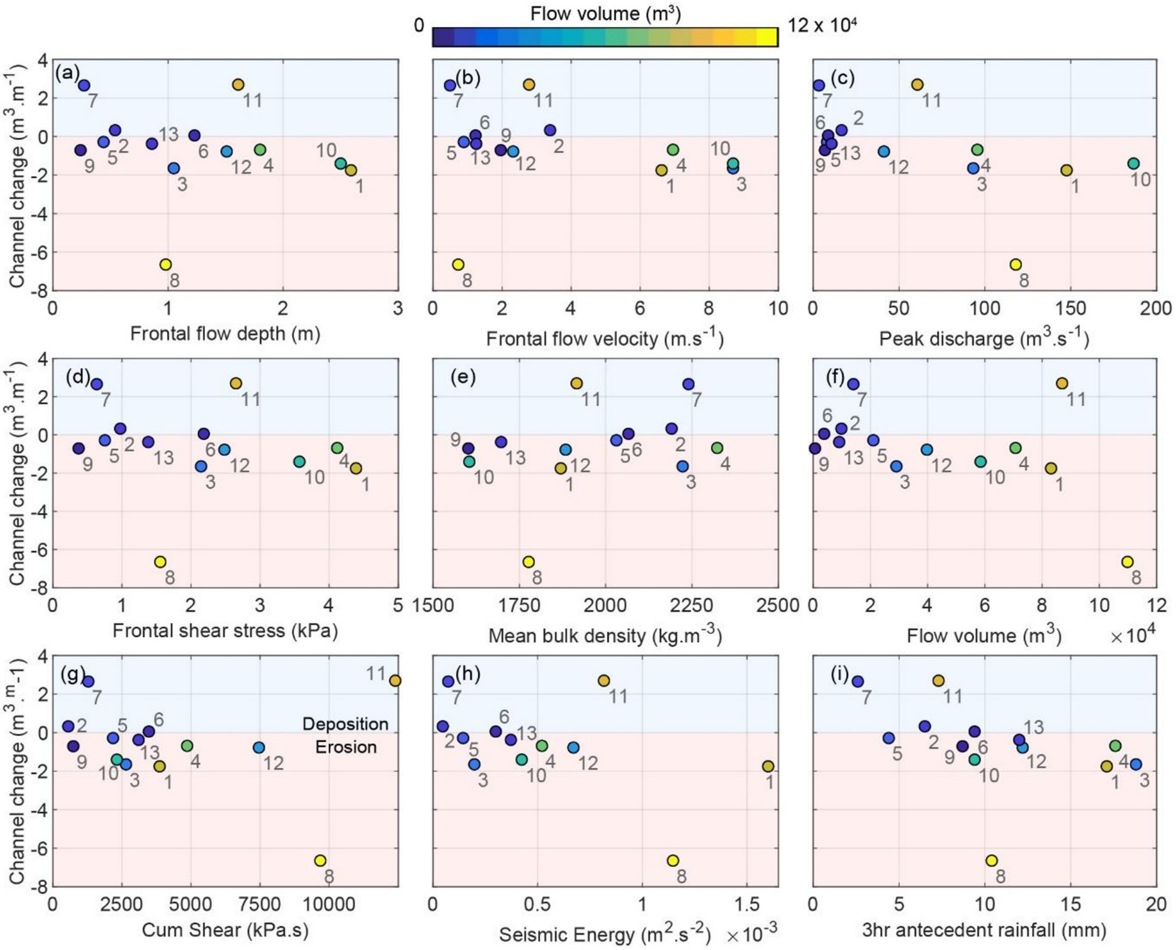

Fig. 3 : Correlations of flow properties (a-h) and antecedent rainfall (i) with channel-bed elevation change (from De Haas et al., [6])

References

1. Frank, F., McArdell, B. W., Huggel, C., Vieli, A. Nat. Hazards Earth Syst. Sci., 15, 2569-2583 (2015).
2. McDougall, S., Hungr, O. Can. Geotech. J., 42, 1437-1448 (2005).
3. Pudasaini, S. P., Krautblatter, M. Nat. Comms., 12, 1-15 (2021).
4. Gregoretti, C., Stancanelli, L. M., Bernard, M., Boreggio, M., Degetto, M., Lanzoni, S. J. Hydrol., 568, 575-591 (2019).
5. de Haas, T., Nijland, W., De Jong, S. M., McArdell, B. W. Sci. Rep., 10, 1-8 (2020).
6. de Haas, T., McArdell, B. W., Nijland, W., Åberg, A. S., Hirschberg, J., Huguenin, P. Geophys. Res. Lett., 49, e2021GL097611.
7. de Haas, T., Nijland, W., McArdell, B. W., Kalthof, M. W. Frontiers in Remote Sensing, 2, 5 (2021).
8. Nota, E. W., Nijland, W., de Haas, T. International Int J Appl Earth Obs Geoinf., 109, 102772 (2022).
9. Schlunegger, F., Badoux, A., McArdell, B. W., Gwerder, C., Schnydrig, D., Rieke-Zapp, D., Molnar, P. Quat. Sci. Rev., 28, 1097-1105 (2009).
10. Iverson, R. M., Reid, M. E., Logan, M., LaHusen, R. G., Godt, J. W., Griswold, J. P. Nat. Geosci., 4, 116-121 (2011).
11. Schürch, P., Densmore, A. L., Rosser, N. J., McArdell, B. W. Geology, 39, 827-830 (2011).
12. McCoy, S. W., Kean, J. W., Coe, J. A., Tucker, G. E., Staley, D. M., Wasklewicz, T. A. J. Geophys. Res. Earth Surf., 117, F03016 (2012).